EARTHQUAKE SIMULATION TESTS OF INDUSTRIAL STEEL STORAGE RACKS

C. K. Chen,[I] R. E. Scholl,[II] and J. A. Blume[III]

SUMMARY

A full-scale industrial steel storage rack was tested on a 20-ft-square shaking table using input motions actually recorded during two California earthquakes. The responses measured during these tests were then compared with results predicted mathematically using various models and procedures. The rack performed well during the tests and was found to be considerably stronger longitudinally than transversely. The predicted responses correlated well with the measured responses.

INTRODUCTION

Industrial steel storage racks are an important class of structures because 40% of all goods are stored on racks at some time during the manufacture-to-consumption cycle. The seismic response behavior of these structures is therefore of significant economic importance and is also important to health and safety in connection with the storage of food and medical supplies. Traditionally, criteria for design and construction of industrial racks have been developed by their manufacturers and have been directed primarily at gravity loading, with little attention given to earthquake loading. This paper is based on a study,[1] by URS/John A. Blume & Associates, Engineers, whose overall objective was to develop seismic design criteria for industrial steel storage racks through correlation and evaluation of the various testing results and analytical parameter variation studies. It summarizes the results of shaking-table tests of one of the three types of racks tested, a full-scale standard pallet rack, and correlates these results with the results predicted theoretically from mathematical models.

TEST STRUCTURE AND INSTRUMENTATION

The standard pallet rack selected for testing is probably the most common rack used for industrial storage. Figure 1 is a photograph of the standard pallet rack assembly on the 20-ft-square shaking table of the University of California, Berkeley.[2] The standard pallet rack modular assembly consists of prefabricated uprights in the transverse direction and horizontal beams spanning between successive uprights in the longitudinal direction. The uprights have two posts 43 in. apart (outside dimensions) that are connected by 96-in.-long horizontal members spaced 5 ft vertically. The upright posts have bearing plates at the bottom that have a single hole, through which floor anchors were installed for the tests considered here. Connections of the upright frame members are tack welded. The beam end connections (shelf connectors) are of the clip-in type, and the upright posts are slotted along their full height to allow variations in beam vertical spacings. The full design live load of 3,000 lb/pallet was simulated by 1,000-lb concrete blocks tied to the beams. All members

---

(I) Project Engineer, (II) Vice President, (III) President, URS/John A. Blume & Associates, Engineers, San Francisco, California

were made of cold-formed steel. The column and brace sections were C-shaped. The data-acquisition system sampled each response channel 50 times per second and stored the results by computer on a magnetic disc; the records were then transferred to magnetic tape for permanent storage. The response quantities measured included accelerations and displacements of each floor and deformations of the columns and the bracing members. Figure 2 shows the test configuration and instrumentation in the longitudinal direction.

TEST RESULTS

Tests were conducted in both the longitudinal direction (semirigid-frame system) and the transverse direction (braced-frame system). The ground motion was simulated by accelerograms recorded during the 1940 El Centro N-S earthquake (EC) and the 1966 Parkfield N65E earthquake (PF). The designations 1/4 EC and 1/2 EC represent tests performed with the maximum amplitude about 1/4 and 1/2 that of the actual El Centro record. Figures 3 and 4 illustrate the 1/2 EC and 1/2 PF input table signals, respectively.

Longitudinal. Eleven test runs were conducted in the longitudinal direction. Selected extreme quantities and dynamic properties are summarized in Table 1a. The variation of dynamic properties with respect to the input signals, amplitudes, and the test sequence is shown in the table. Because of the looseness of semirigid connections, damping values are relatively high. The damping values, which ranged from 3% to 9% of critical, were based on the free-decay data after the table was stopped and free-vibration measurements from previously conducted pull-release tests. The amplification of story shear due to the p-δ effect estimated from the maximum interstory drifts and base shears was found to be very significant in this test direction. The rotation measurements presented for each test clearly demonstrate that the column base provided considerable restraint against rotation, which, in turn, reduced the column moments at the first-story level. The lateral force capacity of this rack configuration was slightly less than that prescribed by the *Uniform Building Code* (*UBC*) Zone 4 lateral force provisions[3] (member capacities were determined using Section 3.6.1 of the American Iron and Steel Institute specifications [AISI 3.6.1]).[4] However, because of the structure's high damping capacity and the early nonlinear behavior at the beam-column connections, the forces developed in the structure by a strong earthquake can be greatly reduced by inelastic action. This behavior was observed in the experiments. With the El Centro earthquake, normalized to a peak of 0.43g in the horizontal direction (about 1.33 EC) and a peak of 0.21g in the vertical direction, the rotational ductility ratio reached 2.6 at the top end of the first-floor center column before minor local distress was observed.

Transverse. Table 1b summarizes the results of some extreme quantities and dynamic response properties from four selected transverse test runs. As expected, the damping or energy-absorbing capacities were smaller (ranging from 1.0% to 1.6% of critical) than those observed in the longitudinal direction. The strong amplitude dependence on the periods of vibration observed in the longitudinal tests was not evident in the transverse tests. Strong localized plastic deformations were observed at the connections between the open-section bracing elements and the open-section columns. This inelastic action might help to reduce the seismic forces

developed in the rack during strong seismic excitation. This localized deformation will significantly affect the response of the rack in the transverse direction. Because of the braced-frame system, the p-δ effect was found to be insignificant. The weakest spots of this rack assembly were the tack welds connecting the columns to the base plates. The tack welds began to fracture at a very low level of excitation (1/4 PF) when the rack was loaded with 2/3 live load. Noticeable distress (buckling) of all columns near their base plates except one at a corner column was observed when the structure was loaded with the full live load under the 1/2 EC input table motion. The estimated maximum rotational ductility ratio at the column near the base plate was approximately 1.9. All strains measured in the bottom diagonals were within the strain yield limit in accordance with AISI 3.6.1, however.

ANALYTICAL CORRELATION

One of the primary objectives of the structural performance shaking table tests was to test the adequacy and effectiveness of various analytical procedures and assumed mathematical models. The computer program DRAIN-2D[5] was used in correlating these procedures and models with the results of the tests.

Longitudinal. Figure 5 shows the mathematical model developed for the standard pallet rack in the longitudinal direction. Semirigid beam-column joints and semifixed column bases[1] were assumed in evaluating stiffness. The p-δ effect was also considered. The bilinear yield mechanism of the moment-rotation relationship for the semirigid connection was idealized as shown in Figure 6. The calculated yield moments of beams and columns are 65 kip-in. and 34 kip-in., respectively. The average column compression force at yield was estimated to be approximately 22 kips in accordance with AISI 3.6.1 and a safety factor of 1.92. Two cases are presented here. For Case 1, the structure was loaded with the full live load and subjected to the input signal of 1/4 PF. Mass-proportional damping corresponding to about 3% of the first-mode viscous damping was assumed for the model. An initial joint rotational spring (K_θ) of 1.4×10^6 lb-in./rad and a moment of inertia of the fictitious floor beams (I_f) of 0.2 in.^{4} were assumed. There was a good correlation (Figure 7), although the predicted rotations were slightly larger than those measured. The response for this case was linear, and no material yielding was detected, either from the analytical or the experimental observations. For Case 2, the model was subjected to the input signal of 1/2 EC. This test run was the first instance in which material yielding at the critical column member was observed from the shaking table tests. Because the data-acquisition system failed at about 12 sec, only response records of 10 sec are included in this presentation. Mass-proportional damping corresponding to about 4.5% of the first-mode viscous damping was prescribed. The parameter K_θ was assigned a value of 10^6 lb-in./rad. Figure 8 shows good agreement between the predicted and measured results. It is apparent that a single basic mathematical model can be used to predict both linear and nonlinear response of the rack structure by varying only damping and joint rotational spring.

Transverse. Figure 9 shows the mathematical model developed in the transverse direction. In modeling this braced-frame system, local deformation at the connections between the braces and column members was considered. The bracing member was treated as a composite. Its stiffness

was reduced as shown in Figure 10. The value of k was assumed and appropriately adjusted[1] in the correlation of measured and predicted results. Two cases are presented here. The Case 1 model was simulated with 2/3 live load and subjected to the input signal of 1/4 EC. Mass-proportional damping corresponding to about 1.5% of the first-mode critical viscous damping was prescribed. The parameters k and I_f were assumed to be 12 and 0.2, respectively. Figure 11 shows the measured and predicted third-floor relative story displacements and bottom diagonal axial strains, which correlate well both in phase and magnitude. For Case 2, the model was loaded with the full live load, and an input earthquake signal of 1/4 PF was applied. All modeling parameters and member properties used in the previous case remained unchanged, with the exception of story mass and input signal. Figure 12 shows measured and predicted results. The correlation was considered good except during the latter stage of response, which was essentially free-decay response. The predicted amplitudes were slightly higher than those observed during the test. These higher results could have been reduced by using a higher damping value in the model. The correlation of analytical results with measured results for these two cases indicates that a single mathematical model can be used to predict seismic responses with different storage weights and input earthquake records.

CONCLUSIONS

The standard pallet rack performed well during the shaking table tests although its lateral force capacity was less than that prescribed in the Zone 4 seismic provisions of the 1976 *UBC*. Because the ductility and energy-dissipation capacity of the racks are much larger in the longitudinal direction than in the transverse direction, the rack can undergo sizable amounts of inelastic deformation in the longitudinal direction without suffering major damage but can only undergo minor amounts of inelastic deformation in the transverse direction. The response predicted theoretically was in good agreement with the experimental results.

ACKNOWLEDGEMENTS

The work described in this paper was supported by the National Science Foundation, the Rack Manufacturers Institute, and the Automated Storage and Retrieval Section of the Material Handling Institute. The assistance of R. W. Clough, who directed the shaking-table tests at the University of California, Berkeley, and of H. W. Krawinkler, who directed the subassembly tests at Stanford University, is greatly appreciated.

REFERENCES

1. Chen, C. K., R. E. Scholl, and J. A. Blume, *Seismic Study of Industrial Steel Storage Racks*, URS/John A. Blume & Associates, Engineers, San Francisco, California (in preparation).
2. Rea, D., and J. Penzien, "Structural Research Using an Earthquake Simulator," *Proceedings*, Structural Engineers Association of California Conference, Monterey, California, 1972.
3. International Conference of Building Officials, *Uniform Building Code*, Whittier, California, 1976.
4. American Iron and Steel Institute, *Specification for the Design of Cold-Formed Steel Structural Members*, New York, 1968.
5. Kanaan, A., and G. H. Powell, *General Purpose Computer Program for Inelastic Dynamic Response of Plane Structures*, EERC 73-5, Earthquake Engineering Research Center, University of California, Berkeley, April 1973 (revised September 1973 and August 1975).

TABLE 1

SUMMARY OF SELECTED EXTREME QUANTITIES AND DYNAMIC PROPERTIES

Live Load	Table Signal	Maximum Table Acceleration (g)		Maximum Table Displacement (in.)	Maximum Third-Level Relative Displacement[a] (in.)	Maximum Interstory Drift (in.)	Maximum Base Shear/Frame		Maximum Base Overturning Moment/Frame (kip-in.)	Maximum Ductility Ratio[c]	Period (sec)[d]			Damping[d] (% Critical)
		Horizontal	Vertical				lb	%[b]			Mode 1	Mode 2	Mode 3	
(a) Longitudinal														
2/3	EC	0.071	--	0.58	1.1	0.57 (0.001H)	434	3.4	62	0.3	1.66 (1.58)	0.43	0.22	(2.9)
2/3	EC	0.166	--	1.33	2.7	1.20 (0.021H)	840	6.6	100	0.7	1.80 (1.66)	0.47	0.22	(4.8)
Full	PF	0.073	--	0.74	2.0	0.93 (0.016H)	800	4.3	90	0.7	2.06 (2.00)	0.53	0.26	(3.6)
Full	EC	0.162	--	1.33	4.4	2.0 (0.034H)	1,200	6.4	145	1.4	2.22 (2.07)	0.53	0.26	(5.5)
Full	PF	0.141	--	1.60	4.3	2.3 (0.040H)	1,150	6.1	125	1.8	2.30 (2.25)	0.57	0.26	(5.5)
Full	EC	0.202	0.110	1.56	4.9	2.4 (0.041H)	1,510	8.1	160	2.2	2.75 (2.35)	0.57	0.27	(9.0)
Full	EC	0.304	0.163	2.27	6.8	3.2 (0.055H)	1,640	8.7	165	2.4	2.86 (2.70)	0.57	0.27	(6.9)
Full	EC	0.431	0.211	3.05	7.3	4.0 (0.069H)	3,600	19.2	252	2.6	2.85 (2.80)	0.57	0.27	(7.6)
(b) Transverse														
2/3	EC	0.073	--	0.61	0.9(W) 1.0(C) 0.9(E)	0.40 (0.007H)	1,120	13.1	150	0.3	0.71 (0.68)	0.24	--	(1.0)
Full	EC	0.077	--	0.62	1.3(W) 1.4(C) 1.3(E)	0.59 (0.010H)	1,650	13.2	200	0.8	0.87 (0.85)	0.28	--	(1.1)
Full	PF	0.077	--	0.80	1.0(W) 1.1(C) 1.0(E)	0.46 (0.008H)	1,200	9.6	160	0.6	0.89 (0.85)	0.30	--	(1.2)
Full	EC	0.158	--	1.29	2.8(W) 2.3(C) 1.8(E)	1.05 (0.018H)	2,550	20.4	280	1.9	0.92 (0.90)	0.30	--	(1.0)
Full	EC	0.200	0.120	1.57	2.5(W) 2.5(C) 2.0(E)	1.10 (0.019H)	2,780	22.2	310	2.1	0.95 (0.92)	0.30	--	(1.6)

a. W = west frame, C = center frame, E = east frame.

b. Percentage of total tributary weight. Longitudinally, ΣW = 18,750 lb (full), 12,750 lb (2/3); transversely, ΣW = 12,500 lb (full), 8,500 lb (2/3).

c. Ductility ratio = ϕ_{max}/ϕ_y, where ϕ_{max} is the maximum measured rotation near the top end (longitudinal) or the base (transverse) of the center bottom column and ϕ_y is the calculated rotation at the initiation of yield.

d. The results shown in parentheses were obtained from decay data from the shaking-table tests.

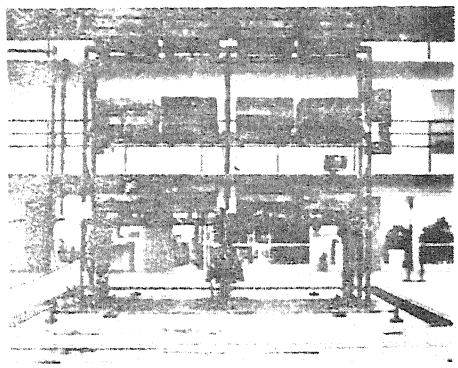

FIGURE 1 TEST STRUCTURE ON SHAKING TABLE

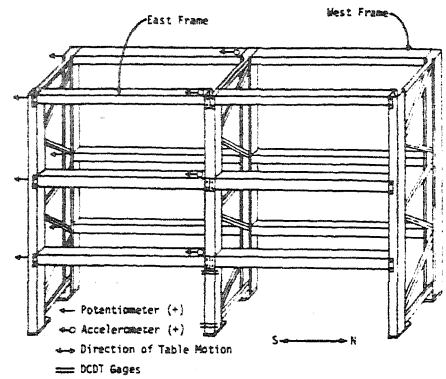

FIGURE 2 LONGITUDINAL TEST CONFIGURATION

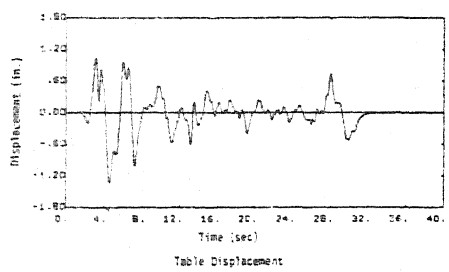

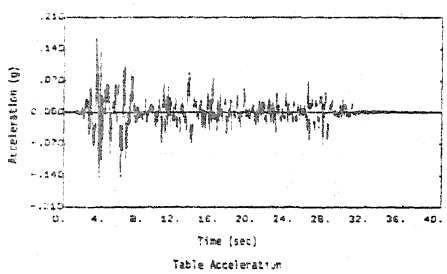

FIGURE 3 TABLE MOTIONS - 1/2 EC

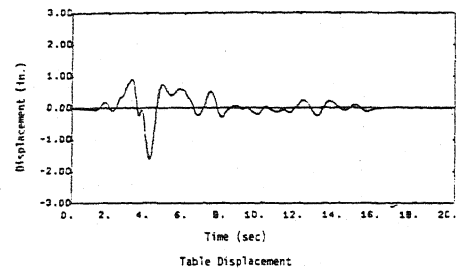

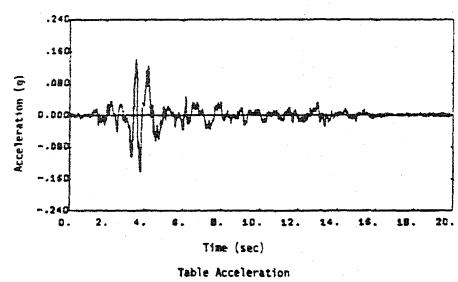

FIGURE 4 TABLE MOTIONS - 1/2 PF

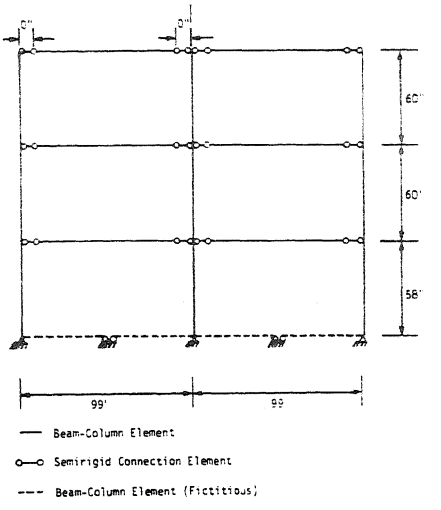

FIGURE 5 MATHEMATICAL MODEL, LONGITUDINAL DIRECTION

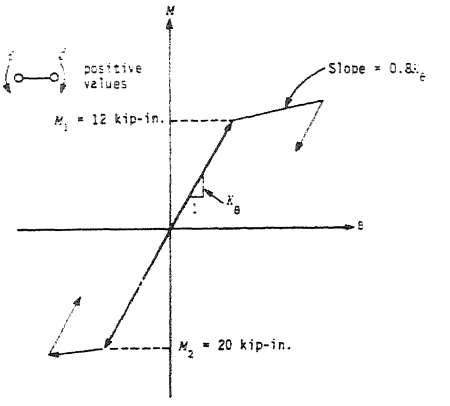

FIGURE 6 MOMENT-ROTATION RELATIONSHIP FOR SEMIRIGID CONNECTION

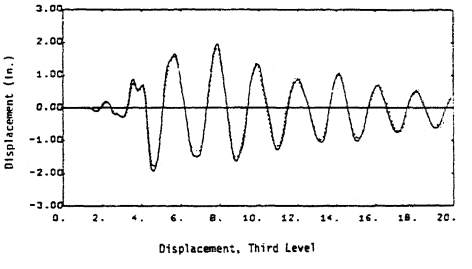

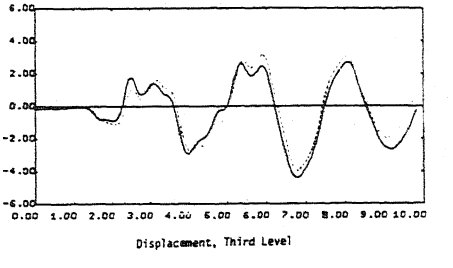

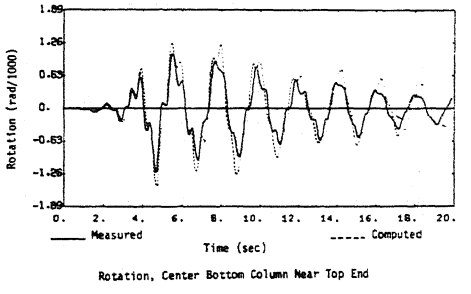

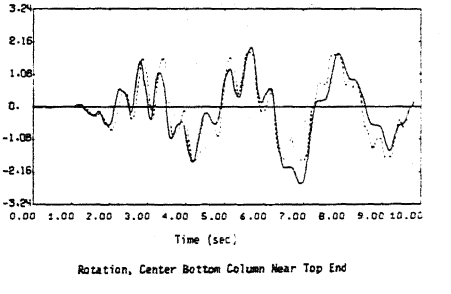

FIGURE 7 COMPUTED AND MEASURED RESULTS - LONGITUDINAL, CASE 1

FIGURE 8 COMPUTED AND MEASURED RESULTS - LONGITUDINAL, CASE 2

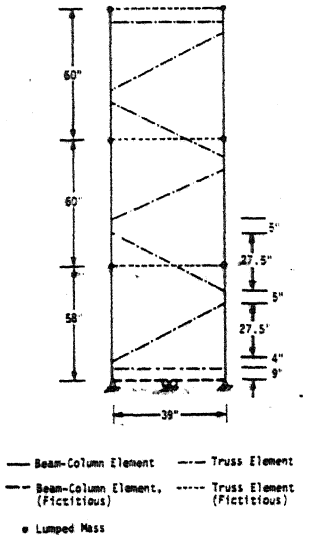

FIGURE 9 MATHEMATICAL MODEL, TRANSVERSE DIRECTION

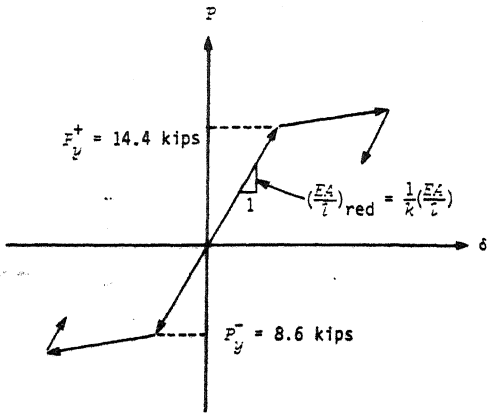

FIGURE 10 BILINEAR YIELD MECHANISM OF DIAGONAL BRACES

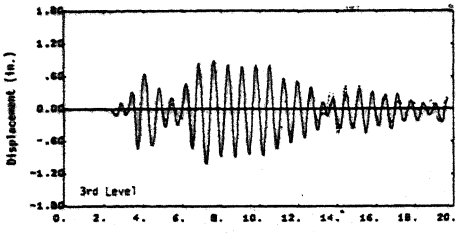

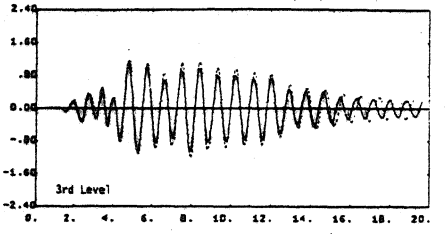

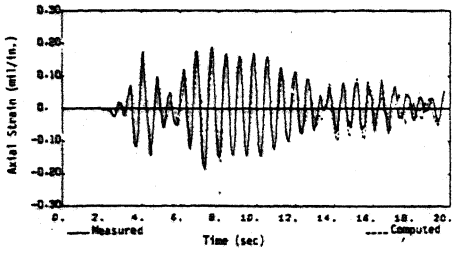

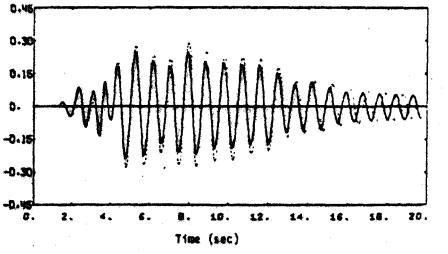

FIGURE 11 COMPUTED AND MEASURED RESULTS - TRANSVERSE, CASE 1

FIGURE 12 COMPUTED AND MEASURED RESULTS - TRANSVERSE, CASE 2